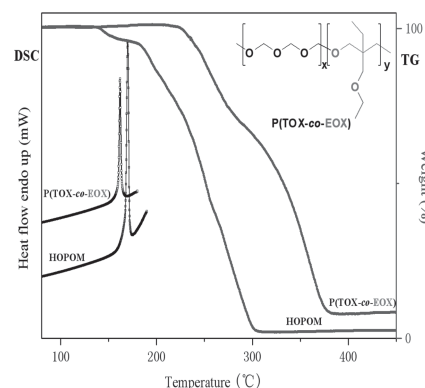


A Novel Branched Polyoxymethylene Synthesized by Cationic Copolymerization of 1,3,5-Trioxane with 3-(Alkoxymethyl)-3-ethyloxetane

Youbing Mu, Mingchen Jia, Wei Jiang, Xiaobo Wan*

Novel branched polyoxymethylene copolymers are synthesized by cationic copolymerization of 1,3,5-trioxane (TOX) with 3-(alkoxymethyl)-3-ethyloxetane (ROX) using $\text{BF}_3 \cdot \text{Et}_2\text{O}$ as an initiator. Four oxetane derivatives with different side-chain lengths (from 1 to 6 carbons) are tested for copolymerization. The copolymer composition is controlled by the feed ratio of ROX, and influenced by the chain length of alkyl group on ROX. The incorporation ratio and side-chain length of the ROX unit have great influence on the thermomechanical properties and crystallinity of the copolymers.



1. Introduction

Polyoxymethylene (POM) is widely used as a traditional metal substitute due to its high crystallinity, and excellent tensile, impact, and compression strength since its discovery in 1920s.^[1] However, because of the thermal

instability of hemiacetal groups at the polymer chain ends, broad use of POM was prevented until the discovery of suitable methods to stabilize the unstable end group.^[2] A common method that has been industrialized is the end-capping reaction of the terminal hemiacetals with acetic anhydride; however, the end-capping process is very energy-intensive, requiring high reaction temperature ($\approx 170^\circ\text{C}$) due to the poor solubility of POM.^[3,4] The other way to improve the thermal stability of POM is by copolymerizing of 1,3,5-trioxane (TOX) with cyclic ethers such as ethylene oxide,^[5–9] 1,3-dioxolane,^[10–13] 1,3-dioxepane,^[14] and 1,3-dioxep-5-ene.^[15] The random introduction of $-\text{[(CH}_2\text{)}_n\text{O]}-$ ($n \geq 2$)— units limits the unzipping of the chain and improves the thermal stability of the $-(\text{CH}_2\text{O})_n-$ units in the copolymer.^[14] Compared with the homopolymer, the resulting copolymers exhibit excellent properties, including lower melting temperature, better alkali and hot water resistance, and better molding processability.^[4] But the copolymerization behavior has remained unclear and is highly related to the properties of the cyclic ethers.^[4,14,16] Besides the cyclic ethers mentioned above, cyclosiloxanes^[17,18] and

Y. Mu, M. Jia, Prof. X. Wan

CAS Key Laboratory of Bio-based Materials, Qingdao Institute of Bioenergy and Bioprocess Technology, Chinese Academy of Sciences, 189 Songling Road, Qingdao, Shandong Province 266101, P. R. China

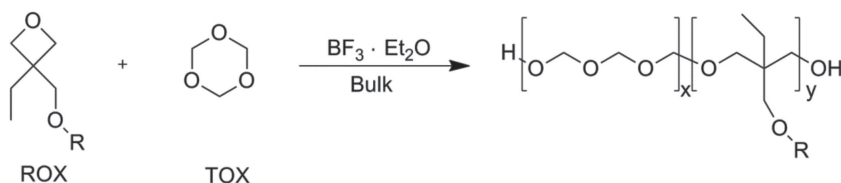
E-mail: wanxb@qibebt.ac.cn

M. Jia

University of Chinese Academy of Sciences, 19A Yuquan Road, Beijing, 100049, P. R. China

Dr. W. Jiang

National Engineering Research Center for Organic Pollution Control and Resource Reuse, State Key Laboratory of Pollution and Resource Reuse, School of the Environment, Nanjing University, 22 Hankou Road, Nanjing, Jiangsu Province, 210093, P. R. China.



■ Scheme 1. Cationic copolymerization of TOX with ROX.

cyclic carbonate^[19] have also been used to copolymerize with TOX. However, although a huge number of papers and patents have been devoted to the copolymerization of various cyclic monomers with TOX, to our surprise, there are only a few patents on the copolymerization of TOX with oxetane derivatives, and no systematic study has been reported on the influence of the incorporate ratio of oxetanes and the length of alkyl side chain on the oxetanes on the thermomechanical properties of the resultant copolymers.^[20–22]

Compared with the liner copolymers of TOX and cyclic monomers without side chains, the branched copolymers of TOX and cyclic monomers with different side chains show greater advantages in the adjustability of their thermomechanical properties, such as melting temperature and melt fluidity.^[23] The introduction of side chains decreases the melting temperature of the resulting polyoxymethylene, which is similar to the melting temperature depression effect of the side chains in linear low-density polyethylenes (LLDPE), but such effect is much smaller in branched POM.^[23,24] It was found that the length of the side chain has little contribution in melting temperature depression of branched POM, and the branch density instead, played a more important role.^[24] Inspired by these results, we turned our attention to oxetane derivatives, which could provide two side chains per monomer thus could introduce higher branch density to the POMs, given that the incorporation ratios are the same. The resulting branched POM may show larger change of thermomechanical properties due to the double side chains in the comonomers. We herein wish to report the synthesis and characterization of the branched POM with 3-(alkoxymethyl)-3-ethyloxetane (ROX) as the comonomers (Scheme 1). One of the side chains of ROX was fixed as ethyl and another side chain was adjustable in length. A series of ROX comonomers with different side-chain lengths were synthesized and copolymerized with TOX to study the influence of incorporation ratio and side-chain length on the thermomechanical properties of the resulting copolymers. The results showed that among all the copolymers, copolymers of TOX and 3-(ethoxymethyl)-3-ethyloxetane (P(TOX-co-EOX)s) show the lowest melting temperature but the best thermal stability, which can be attributed to the higher incorporation ratio of EOX in the copolymers and its moderate side-chain length.

2. Experimental Section

2.1. Materials

TOX was supplied by Risun Coal Chemicals Group (Beijing, China) and purified by recrystallization from ethyl acetate–hexane (V/V = 2/1) and dried under vacuum. All of the other starting materials were purchased

from Sigma–Aldrich and used as received unless otherwise stated. $\text{BF}_3 \cdot \text{Et}_2\text{O}$ was fresh distilled under reduced pressure before use. THF and diethyl ether were dried and distilled before use.

2.2. Instrumentation

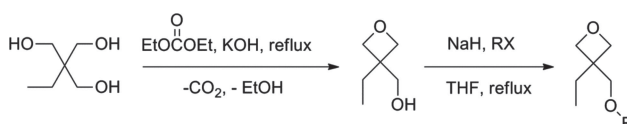
^1H NMR spectra of the copolymers were recorded using a Bruker AV600 spectrometer. The samples for the NMR spectroscopy tests were prepared by dissolving ≈ 10 mg of sample in 0.38 mL of 1,1,1,3,3,3-hexafluoro-2-propanol (HFIP) and adding deuterated chloroform (0.12 mL) as the lock agent. Gel-permeation chromatography (GPC) data were obtained using a Polymer Laboratories PL-GPC20 system with HFIP as the eluent and polystyrene standards (Varian, Inc.). DSC measurements were carried out using an SII DSC-6200 instrument at a heating rate of $10\text{ }^\circ\text{C min}^{-1}$ under a nitrogen atmosphere. The melting temperatures of the cured copolymers were obtained during the second heating cycle. Thermogravimetric analysis (TGA) was performed using a Q500 TGA analyzer by heating the sample using the ramp of $5\text{ }^\circ\text{C min}^{-1}$ from 30 to $600\text{ }^\circ\text{C}$ in a nitrogen flow of 50 mL h^{-1} . Powder X-ray diffraction (XRD) was performed using a Bruker d8 advance X-ray diffractometer with Cu K_α radiation.

2.3. Synthesis of Comonomers

The synthesis route of comonomers is shown in Scheme 2. Four oxetane derivatives were synthesized: 3-ethyl-3-(methoxymethyl) oxetane (MOX), 3-(ethoxymethyl)-3-ethyloxetane (EOX), 3-(butoxymethyl)-3-ethyloxetane (BOX), 3-ethyl-3-((hexyloxy) methyl) oxetane (HOX).

2.3.1. Synthesis of 3-Ethyl-3-hydroxymethyloxetane

The synthesis was performed in a slightly modified procedure reported in the literature.^[25] A mixture of 1,1,1-trihydroxymethylpropane (134.17 g, 1.00 mol), ethylene carbonate (132.6 g, 1.10 mol), and potassium hydroxide (1.0 g in 10 mL of ethanol) was charged into a 500-mL round-bottom flask. The resulting mixture was heated at reflux for 2 h. Ethanol was evaporated at normal atmosphere and the product (80.23 g) was collected at $95\text{--}100\text{ }^\circ\text{C}$ using vacuum fractional distillation. Yield 70%.



■ Scheme 2. Synthesis of 3-ethyl-3-hydroxymethyloxetane and ROX.

^1H NMR (CDCl_3 , 600MHz, δ): 0.90 (t, $J = 6.0$ Hz, 3H; CH_3), 1.73 (q, $J = 6.0$ Hz, 2H; CH_2), 2.41–2.59 (br, 1H), 3.74–3.75 (m, 2H), 4.41 (s, 1H), 4.42 (s, 1H), 4.46 (s, 1H) and 4.47 (s, 1H).

2.3.2. Synthesis of ROX

All the ROX samples were prepared by reacting 3-ethyl-3-hydroxymethyloxetane with the corresponding alkyl halide in the presence of sodium hydride (NaH), following the reported procedure (also shown in Supporting Information).^[25]

MOX was obtained as a colorless liquid using methyl iodide as the reagent (50.00 g, yield 74%). ^1H NMR (CDCl_3 , 600 MHz, δ): 0.88 (t, $J = 6.0$ Hz, 3H; CH_3), 1.74 (q, $J = 6.0$ Hz, 2H; CH_2), 3.39 (s, 3H; CH_3), 3.50 (s, 2H), 4.37 (s, 1H), 4.38 (s, 1H), 4.44 (s, 1H) and 4.45 (s, 1H).

EOX was obtained as a colorless liquid using ethyl bromide as the reagent (50.00 g, yield 67%). ^1H NMR (CDCl_3 , 600 MHz, δ): 0.87 (t, $J = 6$ Hz, 3H; CH_3), 1.18 (t, $J = 6$ Hz, 3H; CH_3), 1.72 (q, $J = 6$ Hz, 2H; CH_2), 3.49 (t, $J = 6.6$ Hz, 2H; CH_2), 3.51 (s, 2H; CH_2), 4.35 (s, 1H), 4.36 (s, 1H), 4.42 (s, 1H) and 4.43 (s, 1H).

BOX was obtained as a colorless liquid using *n*-butyl bromide as the reagent (56.80 g, yield 63.5%). ^1H NMR (CDCl_3 , 600 MHz, δ): 0.86 (t, $J = 7.8$ Hz, 3H; CH_3), 0.90 (t, $J = 7.2$ Hz, 3H; CH_3), 1.35 (m, 2H; CH_2), 1.53 (m, 2H; CH_2), 1.72 (q, $J = 7.2$ Hz, 2H; CH_2), 3.43 (t, $J = 7.8$ Hz, 2H; CH_2), 3.49 (s, 2H; CH_2), 4.34 (s, 1H), 4.35 (s, 1H), 4.41 (s, 1H) and 4.42 (s, 1H).

HOX was obtained as a colorless liquid using *n*-hexyl bromide as the reagent (62.92 g, yield 60.5%). ^1H NMR (CDCl_3 , 600 MHz, δ): 0.85–0.88 (m, 5H), 1.26–1.35 (m, 6H), 1.56 (m, 2H; CH_2), 1.73 (q, $J = 7.2$ Hz, 2H; CH_2), 3.43 (t, $J = 6.6$ Hz, 2H; CH_2), 3.50 (s, 2H), 4.35 (s, 1H), 4.36 (s, 1H), 4.42 (s, 1H) and 4.43 (s, 1H).

2.4. Cationic Copolymerization of TOX and ROX

All the polymerizations were carried in bulk using Schlenk line techniques under a dry Ar atmosphere. General polymerization procedure: TOX (5.0 g, 55.5 mmol) and ROX (various feed fractions) were introduced in a glass tube equipped with a small magnetic stirrer and previously heated in an oven at 80 °C for 30 min under Ar atmosphere. Then, a solution of $\text{BF}_3 \cdot \text{Et}_2\text{O}$ (0.061 g, 0.427 mmol) in anhydrous ether (0.30 mL) was added. The mixture was soon solidified. The mixture was heated at 80 °C for 10 h. After being cooled to room temperature, the polymer was pulled out and extracted with soxhlet extraction in chloroform to remove oligomers and soluble copolymer that mainly contains poly(ROX).

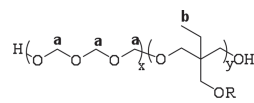
3. Results and Discussion

Oxetane derivatives can be easily obtained from an industrial raw material, 1,1,1-trihydroxy-methylpropane (Scheme 1), which makes them good candidates as the comonomers to adjust the properties of POM. ROX with adjustable length of side chains up to 6 carbons were subjected to study since the copolymerizability of ROX with longer alkyl chain decreases dramatically.

3.1. Cationic Copolymerization of TOX and ROX

Bulk copolymerization, which is the industrialized method to prepare POM, was used to synthesized copolyoxy-methylene. A typical copolymerization experiment of TOX and EOX (entry 6 in Table 1) was carried out at 80 °C in a inert atmosphere in Schlenk tube. The copolymerization occurred almost instantly with very short induction period (less than 5 s) and the solution solidified quickly (less than 2 min). The induction period increases with the increase of the alkyl chain length in ROX. The polymerization was allowed to proceed at this temperature for at least 10 h to guarantee a full conversion. Some of TOX sublimed inevitably and homopolymerized on the upper part wall of the Schlenk tube during the process, and this TOX homopolymer (HOPOM) was carefully removed to avoid any interference with the results. The copolymer was then taken out and subjected to Soxhlet extraction in chloroform several times to remove any homopolymer of oxetanes or the copolymers containing mainly oxetane moieties.^[26] The final copolymer was analyzed by ^1H NMR spectroscopy.



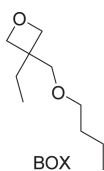
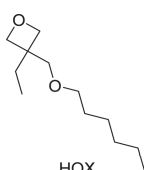
A typical ^1H NMR spectrum of the copolymer with the feeding ratio of TOX:EOX at 70:30 is shown in Figure 1. The signals at 4.80–5.1 ppm are assigned to the methylene protons in the poly(TOX) segments, and the signals at 0.9–3.6 ppm are assigned to the protons in the poly(EOX) segments. The presence of protons from both monomers suggests that the obtained product is indeed copolymer of TOX and EOX. The content ratio of ROX in the copolymer was determined by ^1H NMR spectroscopy according to Equation (1) shown below.^[23] For example, the incorporation ratio is TOX:EOX = 83:17 (Table 1, entry 6) for the copolymers obtained from the feeding ratio at 70:30, which is similar with the copolymers of TOX with 1-ethylene oxide and 4-ethyl dioxolane in previous studies.^[23]


$$\text{mol\%} = \frac{I_{\text{CH}_3}(\text{b})/3}{[I_{\text{CH}_2}(\text{a})/6] + [I_{\text{CH}_3}(\text{b})/3]} \times 100 \quad (1)$$

In Equation (1), $I_{\text{CH}_3}(\text{b})$ is used for the integral of the **b** protons; and $I_{\text{CH}_3}(\text{a})$ is used for the integral of the **a** protons.

The influence of feeding ratio on the copolymerization was studied. The induction period remained in a very short range (from 2.3 to 5 s) when the molar feeding ratio was adjusted from 97:3 (TOX:EOX) to 70:30, but yield of the insoluble copolymer decreases with the increase of EOX feeding content, as shown in Table 1, entry 6–10. This might be partially attributed to that more soluble P(TOX-co-EOX) was extracted with the increase of oxetane content. On the other hand, the incorporation ratio

Table 1. Cationic copolymerization of TOX and ROX.

Entry	ROX	$n_{\text{(T)}}:n_{\text{(O)}} \text{ (O)}^{\text{a}}$ [mol%]	Incorp. O ^{b)} [mol%]	Yield [%]	$T_{\text{m}}^{\text{c)}$ [°C]
P(TOX- <i>co</i> - MOX)					
1 P(TOX ₇₀ - <i>co</i> -MOX ₃₀)	 MOX	70:30(30%)	19.2%	39.2	163.8
2 P(TOX ₈₀ - <i>co</i> - MOX ₂₀)		80:20(20%)	11.5%	46.8	164.9
3 P(TOX ₉₀ - <i>co</i> - MOX ₁₀)		90:10(10%)	5.2%	62.9	165.3
4 P(TOX ₁₉ - <i>co</i> - MOX ₁)		19:1(5%)	4.8%	71.6	167.0
5 P(TOX ₉₇ - <i>co</i> - MOX ₃)		97:3(3%)	2.8%	78.7	168.0
P(TOX- <i>co</i> - EOX)					
6 P(TOX ₇₀ - <i>co</i> - EOX ₃₀)	 EOX	70:30(30%)	16.7%	41.2	161.8
7 P(TOX ₈₀ - <i>co</i> - EOX ₂₀)		80:20(20%)	10.6%	48.1	164.0
8 P(TOX ₉₀ - <i>co</i> - EOX ₁₀)		90:10(10%)	5.2%	60.9	165.8
9 P(TOX ₁₉ - <i>co</i> - EOX ₁)		19:1(5%)	3.3%	68.6	166.9
10 P(TOX ₉₇ - <i>co</i> - EOX ₃)		97:3(3%)	2.4%	75.7	168.1
P(TOX- <i>co</i> - BOX)					
11 P(TOX ₇₀ - <i>co</i> - BOX ₃₀)	 BOX	70:30(30%)	8.3%	32.2	165.6
12 P(TOX ₈₀ - <i>co</i> - BOX ₂₀)		80:20(20%)	4.3%	45.1	166.4
13 P(TOX ₉₀ - <i>co</i> - BOX ₁₀)		90:10(10%)	3.2%	56.9	166.8
14 P(TOX ₁₉ - <i>co</i> - BOX ₁)		19:1(5%)	2.5%	68.1	167.4
15 P(TOX ₉₇ - <i>co</i> - BOX ₃)		97:3(3%)	1.8%	73.7	168.2
P(TOX- <i>co</i> - HOX)					
16 P(TOX ₇₀ - <i>co</i> - HOX ₃₀)	 HOX	70:30(30%)	7.3%	26.2	165.8
17 P(TOX ₈₀ - <i>co</i> - HOX ₂₀)		80:20(20%)	3.1%	31.8	166.3
18 P(TOX ₉₀ - <i>co</i> - HOX ₁₀)		90:10(10%)	2.7%	46.9	166.9
19 P(TOX ₁₉ - <i>co</i> - HOX ₁)		19:1(5%)	2.0%	65.3	167.1
20 P(TOX ₉₇ - <i>co</i> - HOX ₃)		97:3(3%)	1.2%	73.8	167.3

^a)O refers to the ROX, T refers to the TOX; ^b)Determined by ¹H NMR spectroscopy; ^c)Determined by DSC under a N₂ atmosphere.

deviates from the feeding ratio as the EOX feeding content increases. For example, almost all EOX was incorporated into the copolymer (2.4 mol% incorporation ratio) when the TOX/EOX feeding ratio was at 97:3 (entry 10), but only 16.7 mol% of EOX was incorporated when the feeding ratio increased to 70:30 (entry 6).

The copolymerization of TOX and ROX with different alkyl side-chain lengths was also studied. Regardless of the alkyl side-chain length of ROX, similar trend was observed for the yields and incorporation ratio evolution as that observed in EOX. Moreover, under the same feeding ratio, the incorporation ratio of ROX in the copolymer decreases with the increase of the side-chain length. For example, when the feeding ratio is 70:30, incorporation ratio of the MOX unit in the copolymer is 19.2%, but that of the BOX unit is 8.3% (Table 1, entry 1 and 11). The reason for the smaller incorporation ratio might be the decrease of comonomer reactivity. The longer the side

chain of ROX is, the less its copolymerizability with TOX. Nevertheless, the molecular weights and of all the copolymers are around 10 KDa, and the PDI values are quite similar (see Table S1, Supporting Information).

3.2. DSC Measurement

Thermal properties of P(TOX-co-EOX)s were investigated via DSC in a temperature range of 50–190 °C and compared with that of HOPOM, and the results were shown in Figure 2. A main single exothermic peak between 160–180 °C was observed for all the copolymers, which can be associated to the melting process of polymers. The melting temperature of each copolymer was the determined by the exothermic peak temperature and listed in Table 1. In general, for given ROX, melting temperatures of the copolymers decrease with the increase of ROX content, which shows that the incorporation of

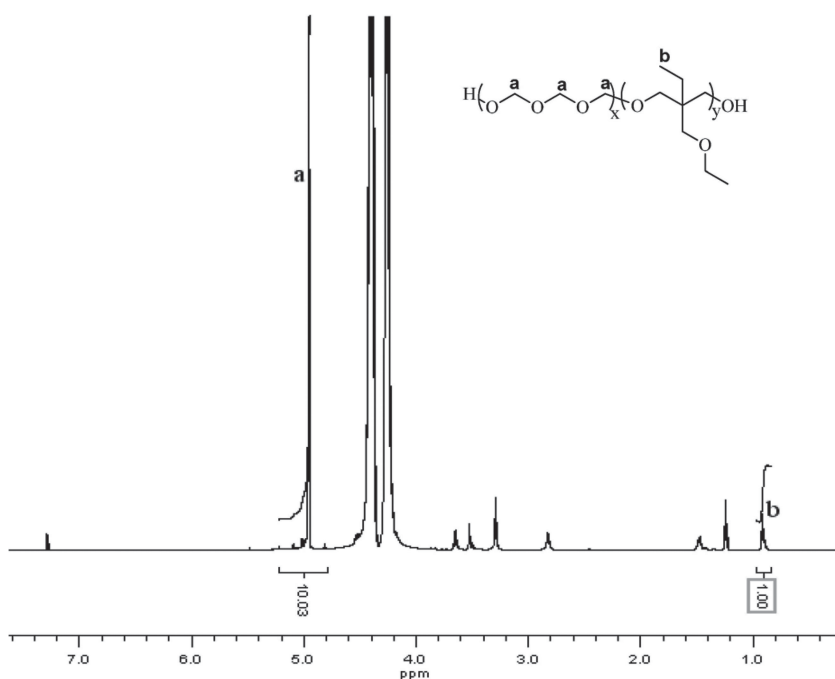


Figure 1. ^1H NMR spectra of the P(TOX₇₀-co-EOX₃₀).

ROX unit impedes crystallization of the copolymer. For example, the melting temperature of P(TOX₇₀-co-MOX₃₀) is 163.8 °C, while the melting temperature of P(TOX₉₇-co-MOX₃) is 168.0 °C. However, considering that the content of MOX increases from 2% to 20% to these two copolymers, the limited decrease (4.2 °C) of the melt temperature demonstrates that the size of the POM crystal cell is not really disturbed by the presence of the comonomer. This might show that the ROX units of the copolymer, even isolated in the chain, do not penetrate the crystal lattice but are rejected into the amorphous phase, due to the steric constraints imposed by the branches. The incorporation of ROX into the main chain leads to the change of volume of the amorphous part, and deeply influences the crystallinity of copolymers.^[27] For different ROXs, the incorporation ratio has to

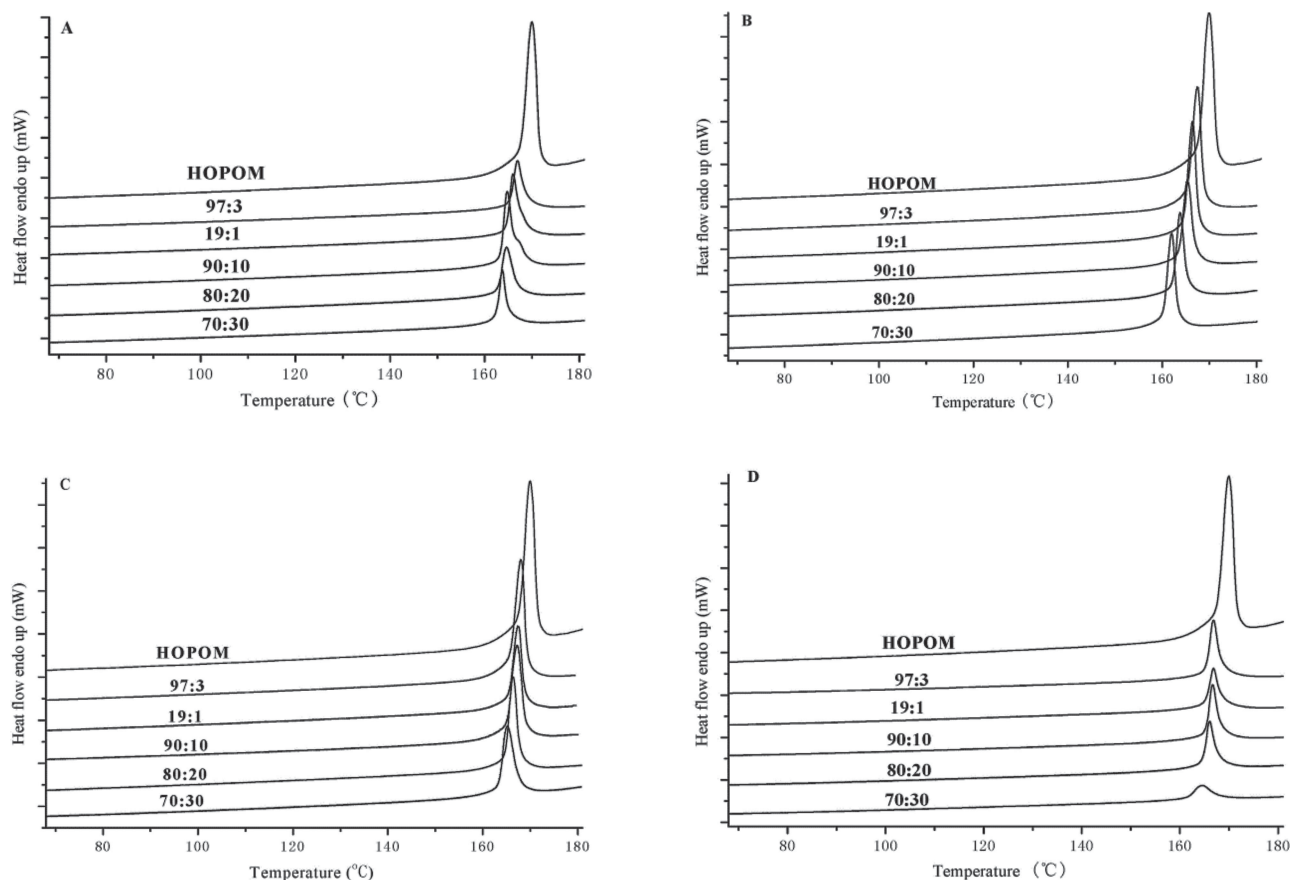


Figure 2. DSC curves of P(TOX-co-ROX): A) copolymers of TOX with MOX; B) copolymers of TOX with EOX; C) copolymers of TOX with BOX; D) copolymers of TOX with HOX. The numbers indicate the initial feed ratios of TOX and corresponding ROX (e.g., 70:30 in A indicates that the initial [TOX:MOX] value is 70:30).

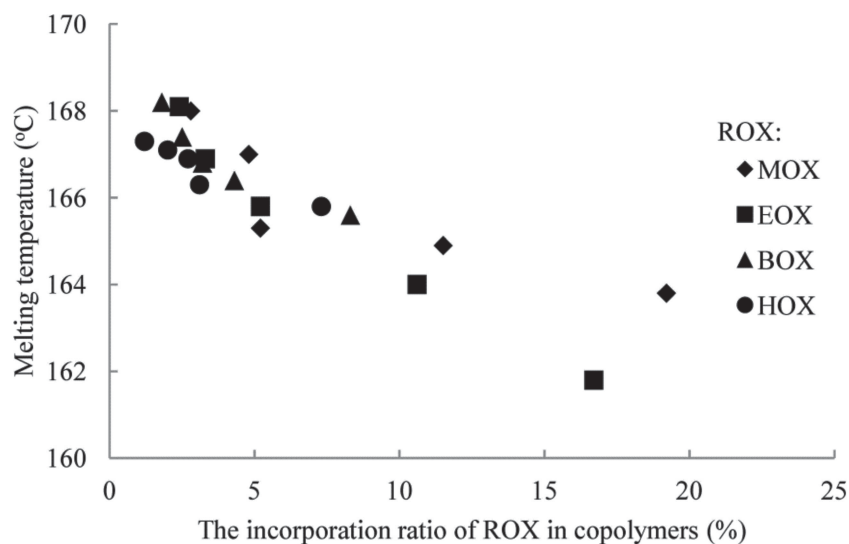


Figure 3. Comparative melting point trends for P(TOX-co-ROX)s based on the incorporation ratio of the ROX unit in the copolymers.

be taken into account to investigate the influence of the side-chain length of ROXs on the melting temperature of the copolymer. Thus, the copolymers with a similar level ($\pm 0.1\%$) of incorporation ratio of the different ROX units were compared. For instance, P(TOX₁₉-co-EOX₁), P(TOX₉₀-co-BOX₁₀), and P(TOX₈₀-co-HOX₂₀) all have a similar incorporation ratio of ROX around 3.2%. The melting temperature of P(TOX₁₉-co-HOX₁) is the lowest (166.3 °C), and that of P(TOX₉₇-co-EOX₃) is the highest (166.9 °C), however, this difference is quite small, which indicates at the same low incorporation ratio, the length of side chain has little effect on the melting temperature of the copolymer. However, at higher incorporation ratio, there might be some side-chain influence on the melting temperature change. For example, For P(TOX₇₀-co-EOX₃₀) with the EOX incorporation ratio at 16.7 mol%, the melting temperature is 2 °C lower than that of P(TOX₇₀-co-MOX₃₀) with the MOX incorporation ratio at 19.2% (Figure 3). This indicates that at high incorporation ratio, EOX has more dramatic melting temperature depression effect than MOX. However, due to the difficulties encountered to incorporate more BOX or HOX units into the copolymer, this effect could not be simply deduced to comonomers with longer side chains. Overall, among all the copolymers, P(TOX-co-EOX) shows best melting temperature depression effect (8.2 °C lower than that of HOPOM), which could be attributed to the higher EOX content in the copolymers and its moderate side-chain length.

3.3. Thermal Stability

Thermal stability of the P(TOX-co-ROX)s was investigated using TGA. Figure 4 presents the overlay of TGA

curves of P(TOX-co-ROX)s with different feed ratio of TOX with ROX. All P(TOX-co-MOX)s and P(TOX-co-EOX)s (Figure 4A,B) demonstrate better thermal stability than HOPOM, which is reflected from the initial decomposition temperature. For example, the initial decomposition temperature of the P(TOX₇₀-co-EOX₃₀) is 227 °C, while that of HOPOM is 157 °C. A 70 °C increase of the decomposition temperature indicates that the incorporation of EOX to the copolymer largely enhanced the thermal stability of the copolymer. In addition, when the temperature is above 300 °C, the HOPOM decomposed completely, but there is still 70% residue left for P(TOX₇₀-co-EOX₃₀) and it is not fully decomposed until the temperature increases to 380 °C. Interestingly,

two decomposition processes are observed in the TGA curves of P(TOX-co-MOX)s and P(TOX-co-EOX)s. A faster decomposition rate is observed at the first stage, and the decomposition rate slows down at the beginning of the second stage. We attributed the first stage to the decomposition of the copolymers with more TOX-rich segments. For example, the weight loss of P(TOX₉₇-co-EOX₃) is about 60% at the first stage, and the rate is quite similar to that of HOPOM. At the second stage, the decomposition rate slows down. With more EOX incorporated into the copolymer, the weight loss at the first stage becomes smaller, for example, only 25% weight loss is observed for P(TOX₇₀-co-EOX₃₀) at the first stage. The second weight loss stage is attributed to the decomposition of the copolymers with more ROX-rich segments. Moreover, the more ROX units incorporated into the copolymer, the higher starting temperature of the second stage is observed. For instance, the second weight loss of P(TOX₉₇-co-EOX₃) starts at 265 °C, while that of P(TOX₇₀-co-EOX₃₀) starts at about 300 °C. This indicates that EOX unit-rich segments are thermally more stable than TOX unit-rich segments. TOX copolymers with 4-alkyldioxolane have been reported in previous study, but the resulting branched acetal copolymers show no improvement on the thermal stability, which can be attributed to the uniformly low comonomer incorporation (0.3–1.6 mol%).^[28] Compared with the P(TOX-co-MOX)s, the initial decomposition temperature of P(TOX-co-EOX)s was higher. For example, the initial decomposition temperature of P(TOX₇₀-co-EOX₃₀) is 227 °C, but that of the P(TOX₇₀-co-MOX₃₀) is 220 °C. It indicates that the EOX unit-rich copolymers are thermally more stable than MOX unit-rich copolymers.

However, all the P(TOX-co-BOX)s and P(TOX-co-HOX)s show even worse thermal stability than HOPOM. Since

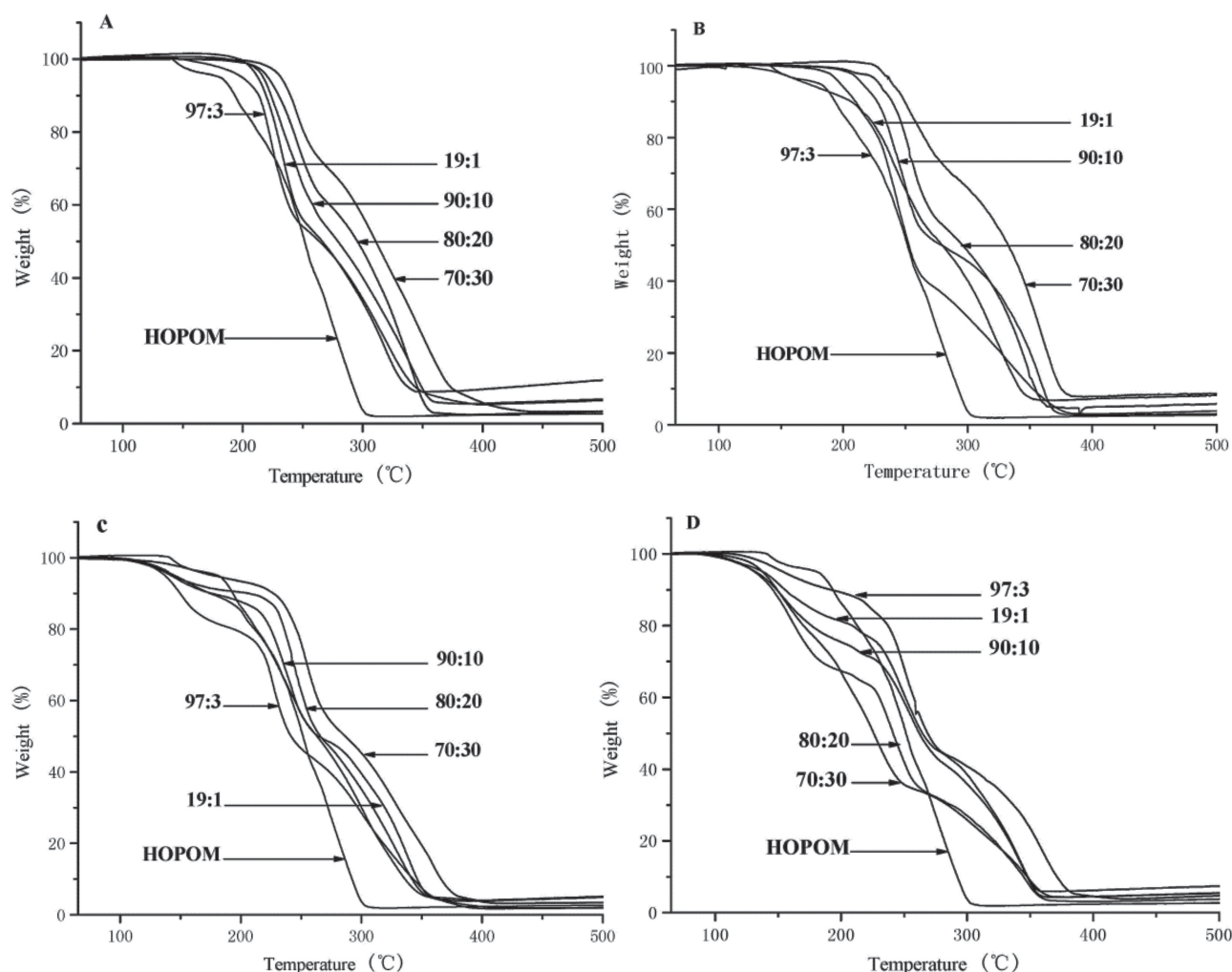


Figure 4. TGA curves of P(TOX-co-ROX): A) copolymers of TOX with MOX; B) copolymers of TOX with EOX; C) copolymers of TOX with BOX; D) copolymers of TOX with HOX. The numbers indicated the initial feed ratios of TOX and corresponding ROX (e.g., 70:30 in A indicates that the initial [TOX:MOX] value is 70:30).

the molecular weights of all the copolymers are quite similar, the influence of the molecular weight on the stability could be ruled out. Three major mass loss stages can be observed in Figure 3C,D. The first decomposition process occurred at the temperature lower than the decomposition temperature of HOPOM. This may be due to the two possible reasons: first, the lower incorporation ratio of BOX or HOX unit in the copolymers (Table 2) leads to the less thermal stability than P(TOX-co-MOX)s and P(TOX-co-EOX)s. Second, the longer side-chain (butyl and hexyl) make the backbone of copolymers become more loosely packed and may lead to the exposure of the $(-\text{CH}_2-\text{O})_n$ unit and the hemiacetal group to the outside environment, which might be pyrolyzed at lower temperature.

Nevertheless, the thermal stability of P(TOX-co-BOX)s showed similar trend as P(TOX-co-MOX)s and P(TOX-co-EOX)s, which increases with the increase of ROX content (Figure 4C). However, a reverse trend was observed in

P(TOX-co-HOX) (Figure 4D). It implies that alkyl side chain longer than 4 carbons on ROX has an adverse effect on the thermal stability of the resulting copolymer. In conclusion, the changes of melt temperature and thermal stability of branched POM are the result of a combination of incorporation ratio of the ROX unit and side-chain length of comonomers.

3.4. XRD Study of the Copolymers

The powder XRD patterns of HOPOM and P(TOX₇₀-co-ROX₃₀) were investigated and shown in Figure 5 (XRD of all P(TOX-co-EOX) copolymers are shown in Figure S25 in the Supporting Information). All of the copolymers show a sharp peak at $2\theta = 23^\circ$, which is assigned to the crystalline POM region, and an obvious broad peak at $2\theta = 21^\circ$, which is assigned to the amorphous region. The crystallinity was then calculated from the X-ray diffraction pattern

Table 2. Crystallinity of polymers.

Polymer	Crystallinity [%]
HOPOM	94
P(TOX ₉₇ -co-EOX ₃)	91
P(TOX ₁₉ -co-EOX ₁)	88
P(TOX ₉₀ -co-EOX ₁₀)	82
P(TOX ₈₀ -co-EOX ₂₀)	78
P(TOX ₇₀ -co-EOX ₃₀)	70
P(TOX ₇₀ -co-MOX ₃₀)	67
P(TOX ₇₀ -co-BOX ₃₀)	61
P(TOX ₇₀ -co-HOX ₃₀)	57

of the range of $2\theta = 8\text{--}30^\circ$. The crystalline peak and the amorphous peak were separated by the Gaussian approximation.^[7] The amplified peak charts are also shown in Figure 5 (original drawing is shown in Figure S24 in the Supporting Information) and a summary of the crystallinity of the copolymers is shown in Table 2.

For all the P(TOX-co-EOX) samples, the crystallinity decreases with increase of the incorporation ratio of EOX unit in the copolymers, as shown in Table 2. It is consistent with the change of melt temperature and thermal stability of all P(TOX-co-EOX)s (Figure 2B). For all the P(TOX₇₀-co-ROX₃₀), the crystallinity (70%) is lower than the copolymers of TOX and cyclic ethers reported in previous study,^[7,12] which can be due to the higher incorporation ratio of the ROX unit and double side chains of comonomers. Among the P(TOX₇₀-co-ROX₃₀) samples, P(TOX₇₀-co-EOX₃₀) shows the highest crystallinity (70%), which sug-

gests that the incorporation ratio of both the ROX unit and side-chain length of comonomers affects the crystallinity. This order of crystallinity is also in accordance with the observation that the P(TOX-co-EOX) samples have the best thermal stability among the P(TOX-co-ROX)s (Figure 4). On the other hand, although P(TOX₇₀-co-EOX₃₀) shows the highest crystallinity, it has the lowest melting temperature (161.8 °C), which suggests that crystallinity is not the only determining factor for the melting temperature of branched crystalline copolymers.

4. Conclusion

Copolymers of TOX with oxetane derivatives with different side chains were synthesized via bulk cationic ring-opening copolymerization. The side-chain length of ROX remarkably affects the incorporation ratio of ROX in the copolymer, that is, the longer the side chain of ROX, the fewer the ROX units in the copolymer. DSC, TG, and XRD analyses of the copolymers indicate that the incorporation ratio of the ROX unit in the copolymers and the side-chain length of comonomers have a great effect on the thermo-mechanical properties and crystallinity. The changes of melting temperature and thermal stability of branched POM are the result of a combination of incorporation ratio of the ROX unit and the side-chain length of the comonomers. Oxetanes with shorter side-chain lengths not only display increased copolymer thermostability, but also display a lower melting temperature. On the other hand, although oxetanes with longer side-chain length could also lower their melting temperature of the copolymers, the thermostability could not be improved. Among

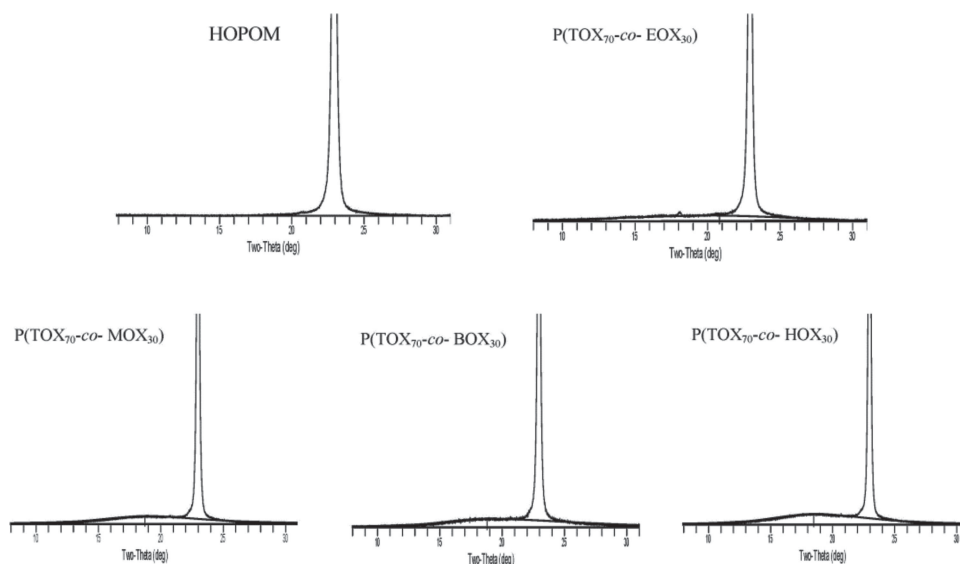


Figure 5. XRD patterns of P(TOX₇₀-co-ROX₃₀).

all the copolymer studied, P(TOX-co-EOX) exhibited the best thermostability and the lowest melting temperature, which should improve the processability of the copolymer. Further work is needed to understand the copolymerization mechanism and to further improve the thermostability and processability of the copolymer.

Supporting Information

Supporting Information is available from the Wiley Online Library or from the author.

Acknowledgements: The authors thank the financial support from the “100 Talents” program from the Chinese Academy of Sciences.

Received: July 18, 2013; Revised: August 13, 2013; Published online: September 16, 2013; DOI: 10.1002/macp.201300473

Keywords: cationic polymerization; 3-(alkoxymethyl)-3-ethyloxetane; copolymerization; polyoxymethylene; thermal properties

- [1] M. Dröschner, G. Wegner, *Ind. Eng. Chem. Product Res. Dev.* **1979**, *18*, 259.
- [2] S. H. Jenkins, J. O. Punderson, US Patent 2 964 500, **1960**.
- [3] J. Masamoto, T. Iwaisako, K. Matsuzaki, *J. Macromol. Sci., Part A* **1992**, *29*, 441.
- [4] J. Masamoto, *Prog. Polym. Sci.* **1993**, *18*, 1.
- [5] H. Nagahara, K. Kagawa, K. Hamanaka, K. Yoshida, T. Iwaisako, J. Masamoto, *Ind. Eng. Chem. Res.* **2000**, *39*, 2275.
- [6] N. Yamasaki, K. Kanaori, J. Masamoto, *J. Polym. Sci., Polym. Chem.* **2001**, *39*, 3239.
- [7] K. Matsuzaki, M. Maeda, M. Kondo, H. Morishita, M. Hamada, T. Yamaguchi, K. Neki, J. Masamoto, *J. Polym. Sci., Part A: Polym. Chem.* **1997**, *35*, 2479.
- [8] J. Masamoto, K. Matsuzaki, *Macromol. Symp.* **1998**, *132*, 431.
- [9] S. Turri, A. Sanguineti, M. Levi, *Macromol. Chem. Phys.* **1997**, *198*, 3215.
- [10] K. Beloufa, N. Sahli, M. Belbachir, *J. Appl. Polym. Sci.* **2010**, *115*, 2820.
- [11] Y. T. Shiehl, M. L. Lay, S. A. Chen, *J. Polym. Res.* **2003**, *10*, 10.
- [12] L. H. Sun, Z. G. Yang, X. H. Li, *J. Appl. Polym. Sci.* **2008**, *107*, 1842.
- [13] P. J. Holdsworth, E. W. Fischer, *Makromol. Chem.* **1974**, *175*, 2635.
- [14] K. Sharavanan, E. Ortega, M. Moreau, C. D. Lorthioir, F. O. Laupretre, P. Desbois, M. Klatt, J. P. Vairon, *Macromolecules* **2009**, *42*, 8702.
- [15] R. A. Rodriguez, S. Wang, N. L. Yang, A. Auerbach, J. Paul, *Die Makromol. Chem.* **1990**, *191*, 99.
- [16] In *Cationic Ring-Opening Polymerization*, (Eds: S. Penczek, P. Kubisa, K. Matyjaszewski), Springer, Berlin, Heidelberg, Germany **1985**, p. 91.
- [17] M. R. Baeza, M. Zapata, *Polym. Bull.* **1996**, *36*, 7.
- [18] M. R. Baeza, M. Zupata, *Macromol. Rapid Commun.* **1997**, *18*, 8.
- [19] D. Nagai, K. Yokota, T. Ogawa, B. Ochiai, T. Endo, *J. Polym. Sci., Part A: Polym. Chem.* **2008**, *46*, 733.
- [20] K. Kullmar, F. A. Main, K. Gutweiler, Mainz, M. Weissermel, DE Patent 1 196 374, **1960**.
- [21] D. Kobayashi, A. Okamura, JP Patent 266 372, **2008**.
- [22] T. Yoshihisa, JP Patent 275 227, **2002**.
- [23] A. D. Ilg, C. J. Price, S. A. Miller, *Macromolecules* **2007**, *40*, 7739.
- [24] R. T. Martin, S. A. Miller, *Macromol. Symp.* **2009**, *279*, 72.
- [25] J. V. Crivello, H. Sasaki, *J. Macromol. Sci., Part A* **1993**, *30*, 189.
- [26] H. Boucekif, M. I. Philbin, E. Colclough, A. J. Amass, *Macromolecules* **2008**, *41*, 1989.
- [27] C. Lorthioir, F. Laupretre, K. Sharavanan, R. F. M. Lange, P. Desbois, M. Moreau, J. P. Vairon, *Macromolecules* **2007**, *40*, 5001.
- [28] D. Braun, U. Brückner, P. Eckardt, M. Hoffmockel, *Angew. Makromol. Chem.* **1999**, *265*, 55.